Journal of Molecular and Cellular Cardiology 129 (2019) 219–230

Contents lists available at ScienceDirect

Journal of Molecular and Cellular Cardiology

journal homepage: www.elsevier.com/locate/yjmcc

Original article

Activation of the cation channel TRPM3 in perivascular nerves induces vasodilation of resistance arteries

Lucía Alonso-Carbajo[a,b], Yeranddy A. Alpizar[a], Justyna B. Startek[a], José Ramón López-López[b], María Teresa Pérez-García[b], Karel Talavera[a,*]

[a] Department of Cellular and Molecular Medicine, Laboratory of Ion Channel Research, KU Leuven, VIB Center for Brain & Disease Research, Herestraat 49, Campus Gasthuisberg, O&N1 Box 802, 3000 Leuven, Belgium

[b] Departamento de Bioquímica y Biología Molecular y Fisiología, Instituto de Biología y Genética Molecular, Universidad de Valladolid y CSIC, Sanz y Forés 3, 47003 Valladolid, Spain

ARTICLE INFO

Keywords:
TRPM3
Perivascular nerve
Vasodilation
Pregnenolone sulfate
CGRP

ABSTRACT

The Transient Receptor Potential Melastatin 3 (TRPM3) is a Ca^{2+}-permeable non-selective cation channel activated by the neurosteroid pregnenolone sulfate (PS). This compound was previously shown to contract mouse aorta by activating TRPM3 in vascular smooth muscle cells (VSMC), and proposed as therapeutic modulator of vascular functions. However, PS effects and the role of TRPM3 in resistance arteries remain unknown. Thus, we aimed at determining the localization and physiological role of TRPM3 in mouse mesenteric arteries. Real-time qPCR experiments, anatomical localization using immunofluorescence microscopy and patch-clamp recordings in isolated VSMC showed that TRPM3 expression in mesenteric arteries is restricted to perivascular nerves. Pressure myography experiments in wild type (WT) mouse arteries showed that PS vasodilates with a concentration-dependence that was best fit by two Hill components (effective concentrations, EC_{50}, of 14 and 100 μM). The low EC_{50} component was absent in preparations from *Trpm3* knockout (KO) mice and in WT arteries in the presence of the CGRP receptor antagonist BIBN 4096. TRPM3-dependent vasodilation was partially inhibited by a cocktail of K^+ channel blockers, and not mediated by β-adrenergic signaling. We conclude that, contrary to what was found in aorta, PS dilates mesenteric arteries, partly via an activation of TRPM3 that triggers CGRP release from perivascular nerve endings and a subsequent activation of K^+ channels in VSMC. We propose that TRPM3 is implicated in the regulation of the tone of resistance arteries and that its activation by yet unidentified endogenous damage-associated molecules lead to protective vasodilation responses in mesenteric arteries.

1. Introduction

Several members of the Transient Receptor Potential (TRP) protein superfamily have been recently identified in vascular smooth muscle, endothelial and perivascular cells, and their study is an emerging theme in cardiovascular research [1,2]. TRP proteins form cation channels, and with the exceptions of TRPM4 and TRPM5, all of them permeate Ca^{2+} [3]. TRP channel activation can thus directly affect Ca^{2+}-dependent signaling and modulate the membrane potential, and thereby the function of voltage-gated K^+ and Ca^{2+} channels that ultimately determine the vascular tone. There are substantial discrepancies about TRP channel functions in the vascular system, most of which arise from the lack of appropriate pharmacological tools and the difficulty of studying these channels in native cellular conditions [2]. Yet, several TRP channels have been implicated in the regulation of the vascular tone via multiple mechanisms. For instance, TRPC channels were identified as receptor-operated or store-operated Ca^{2+} entry channels in vascular smooth muscle cells (VSMC) [4,5], activation of TRPV4 in

Abbreviations: AC, Adenylate cyclase; α-SMA, Alpha-smooth muscle actin; β-gal, β-Galactosidase; cAMP, cyclic adenosine monophosphate; CGRP, Calcitonin gene-related peptide; EC, Endothelial cells; GAPDH, Glyceraldehyde 3-phosphate dehydrogenase; HEK293T, Human embryonic kidney cell 293 SV40 T-antigen; KO, Knockout; NA, Noradrenaline; NF-200, Neurofilament 200; PGP9.5, Protein gene product 9.5; PKA, Protein kinase A; PS, Pregnenolone sulfate; SMDS, Smooth muscle dissociation solution; TH, Tyrosine hydroxylase; TRP, Transient receptor potential; TRPM, Transient receptor potential melastatin; UTP, Uridine-5′-triphosphate; VSMC, Vascular smooth muscle cells

* Corresponding author at: Laboratory of Ion Channel Research, Dept. of Cellular and Molecular Medicine, KU Leuven, Herestraat 49, Campus Gasthuisberg, O&N1 Box 802, B-3000 Leuven, Belgium.

E-mail address: karel.talavera@kuleuven.vib.be (K. Talavera).

https://doi.org/10.1016/j.yjmcc.2019.03.003
Received 7 January 2019; Received in revised form 1 March 2019; Accepted 6 March 2019
Available online 07 March 2019
0022-2828/ © 2019 Elsevier Ltd. All rights reserved.

VSMC and endothelial cells (EC) induces vasodilation [6,7], and TRPV1 and TRPA1 contribute to vasodilation mediated by stimulation of perivascular sensory nerves [8,9].

The role of the melastatin family of TRP channels (8 members, TRPM1 to TRPM8) in vascular function remains ill-defined in most cases. TRPM4 has been shown to participate in the myogenic response of cerebral arteries [10], but seems to be absent in other resistance arteries [11]. TRPM2 is expressed in EC and regulates endothelial permeability [12], while TRPM6 and TRPM7 have been found in VSMC as critically involved in Mg^{2+} homeostasis [13]. Regarding TRPM3 [14–16], it has only recently been described mRNA and protein expression in mouse aorta and human saphenous veins [17]. Activation of TRPM3 by the steroid pregnenolone sulfate (PS) was reported to induce aortic contraction, as deduced from the inhibitory effects of antibodies blocking this channel. However, multiple key questions on the role of TRPM3 to vascular function remain open. First, the specificity of PS as TRPM3 agonist in vascular tissue has not been tested with the use of *Trpm3* knockout (KO) mice. Second, the contributions of TRPM3 to the tone of resistance arteries and to the regulation of blood pressure are still unknown. Recent findings unveiling TRPM3 as thermo-sensor and potential chemo-sensor in nociceptive neurons [18,19] suggest that, if present in perivascular nerve endings, activation of this channel might result in neuropeptide release. This would suppose a vasodilating effect of TRPM3 activation, an action opposite to the vasoconstriction previously described in mouse aorta [17].

In order to address these questions, we first investigated the localization of TRPM3 in mouse mesenteric arteries. Next, we performed myography experiments in arteries isolated from wild type (WT) and *Trpm3* KO mice to determine the specificity of PS and to characterize the mechanism of action of this compound. We found that, contrary to what was reported for aorta [17], PS induces vasodilation of mesenteric arteries, and that these effects are partly mediated by activation of TRPM3, via release of CGRP and subsequent activation of K^+ channels in VSMC. Our data support a contribution of TRPM3 as a potential therapeutic target for the modulation of the tone of resistance arteries and as a plausible effector of endogenous damage-associated molecules mediating protective responses in these vascular beds.

2. Methods

2.1. Mice

The experiments were performed on WT C57bl/6J (Janvier Laboratories, Saint-Berthevin Cedex, France) and *Trpm3* KO male mice weighing about 25 g and from 10 to 12 weeks of age. They received standard food and drinking water ad libitum. Animals were anesthetized and then euthanized by CO_2 inhalation. The *Trpm3* KO mice are global knockouts produced by the insertion of a cassette containing a beta-geo fusion construct flanked by a 5′-terminal IRES sequence into exon 17 of the mouse *Trpm3* gene by homologous recombination [19,20]. These mice have a decreased sensitivity to heat [19], but are otherwise viable, fertile, and exhibit no differences from WT animals in terms of general appearance and gross anatomy. All protocols were in accordance with the European Community and Belgian Governmental guidelines for the use and care of experimental animals (2010/63/EU, CE Off Jn8L358, LA12110551) and approved by the KU Leuven Ethical Committee Laboratory Animals (ECD) and the Institutional Care and Use Committee of the University of Valladolid.

2.2. Isolation of VSMC

Segments of third-order mesenteric arteries were dissected and cleaned of adipose tissue in cold oxygenated smooth muscle dissociation solution (SMDS-10 μM Ca^{2+}) containing (in mM): 145 NaCl, 4.2 KCl, 0.6 KH_2PO_4, 1.2 $MgCl_2$, 10 HEPES, glucose 11 (pH 7.4, adjusted with NaOH) and 10 μM $CaCl_2$. The dissected arteries were subjected to two consecutive processes of enzymatic digestion in order to isolate VSMC. The first digestion was carried out at 37 °C for 14–16 min in SMDS-Ca^{2+}-free solution containing 0.8 mg/ml papain (Worthington Biochemical Corp.), 1 mg/ml BSA (Sigma-Aldrich) and 1 mg/ml dithiothreitol (Sigma-Aldrich). The second digestion was performed at 37 °C for 14–16 min using SMDS-10 μM Ca^{2+} supplemented with 0.6 mg/ml collagenase F (Sigma-Aldrich) and 1 mg/ml BSA. Digested arteries were rinsed twice with SMDS-10 μM Ca^{2+}. After this washing step, single cells were obtained by mechanical disruption with a wide-bore glass pipette. Cells were maintained at 4 °C until they were used in patch-clamp recordings.

2.3. qRT – PCR analyses

Mesenteric arteries were enzymatically digested as described in the previous section, but decreasing the incubation time to 8–10 min with the enzymes and skipping the washing step with SMDS-10 μM Ca^{2+}, so that nerve fibers, smooth muscle and endothelial cells were still present in the preparation. Arteries of 6 mice were used for each determination. Total RNA from the digested arteries was extracted using RNeasy mini kit (Qiagen), following the manufacturer's protocol. cDNA synthesis was performed with 500 ng of total RNA of the previous step using Ready-to-go First strand beads (GE Healthcare). A small fraction of the cDNAs was used for quantitative real-time PCR. Each qPCR reaction (20 μl) contained 3 μl of cDNA template, 10 μl of Universal TaqMan MasterMix (2× concentrated, Life Technologies), 1 μl of TaqMan probe (Table 1, 20× concentrated, Life Technologies) and 6 μl H_2O. For every experiment, test reactions were performed in triplicate, and non-template negative controls in duplicate. Fluorescent signals generated during PCR amplifications were normalized to an internal reference (GAPDH). The threshold cycle (Ct) was set within the exponential phase, and the relative quantitative evaluation of target gene levels was performed using the $2^{-\Delta Ct}$ method. Differences between samples with and without endothelium were calculated as $2^{-\Delta\Delta Ct}$, where $\Delta\Delta Ct = \Delta Ct_{without} - \Delta Ct_{with}$.

2.4. Immunofluorescence microscopy

Intact arteries were fixed with 4% paraformaldehyde (PFA) in PBS for 15 min, permeabilized in PBTx (PBS, 0.2% Triton X-100) and blocked with PBTx with 2% of sheep serum for 3 h. Arteries were incubated overnight at 4 °C with the primary rabbit anti-TRPM3 (1:100, Santa Cruz), mouse anti-NF-200 (1:1000, Alomone), human anti-PGP9.5 (1:100, Santa Cruz), chicken anti-β-gal IgY (1:1000, Abcam), rabbit anti-calcitonin gene-related peptide (1:500, Abcam), mouse anti-tyrosine hydroxylase (1:1000, Abcam) or rabbit anti-alpha smooth muscle actin (1:250, Abcam) antibodies, followed by the secondary antibodies Alexa 594 goat anti-rabbit (1:1000, Molecular Probes), Alexa 555 anti-mouse (1:1000, Abcam), 488 donkey anti-chicken or goat anti-chicken IgY-Alexa 488 (1:1000, Abcam). Secondary antibodies were prepared in blocking solution and incubated for at least 2 h at room

Table 1
List of TRP-specific TaqMan gene expression assays (Life Technologies).

Gene name	Assay ID	GenBank mRNA	Exon boundary	Assay location	Amplicon length
TRPM1	Mm00450619	AF047714.1	6–7	822	90
TRPM2	Mm00663098	AB166747.1	29–30	4265	107
Trpm3	Mm00616485	AK051867.1	21–22	3135	75
Trpm4	Mm00613173	AJ575814.1	9–10	1204	78
Trpm5	Mm00498453	AB039952.1	18–19	2787	73
Trpm6	Mm00463112	AK080899.1	13–14	1520	125
Trpm7	Mm00457998	AY032951.1	13–14	1752	125
Trpm8	Mm00454566	AF481480.2	24–25	3389	89
Gapdh	4352932E	NM008084.2	–	–	107

temperature. Finally, the arteries were flat-mounted in glass slides using DAPI-containing mounting solution (VectaShield, Vector Laboratories).

HEK293T cells were plated in polyL-lysine-coated coverslips, fixed with 4% PFA in PBS for 15 min and blocked with PBS with 2% of sheep serum for 3 h. The cells were incubated with primary antibody rabbit anti-TRPM3 (1:100, Santa Cruz) overnight at 4 °C. After that, samples were incubated with the secondary antibody Alexa 594 goat anti-rabbit (1:1000, Molecular Probes) in blocking solution during 2 h at 22 °C. The coverslips were mounted using DAPI-containing mounting solution (VectaShield, Vector Laboratories).

Confocal images of labeled cells and arteries were collected using the optimal pinhole size for the Plan-Apochromat 63 × /1.4 oil objective and 20 × or 40 × objective of a Zeiss LSM 510 Meta Multiphoton microscope (Carl Zeiss AG). Images were acquired by consecutive excitation with an Argon laser at 488 nm and He-Ne laser at 543 nm. For nuclear DAPI staining, we used a two-photon pulsed excitation by the Spectra-Physics (Mountain View) Mai Tai laser at 770 nm. Images were analyzed using ImageJ processing software.

2.5. Patch-clamp electrophysiology

Whole-cell patch-clamp recordings were performed in freshly isolated VSMC at ~22 °C using an Axopatch 200 patch-clamp amplifier (Axon Instruments, Molecular Devices), filtering at 2 kHz (−3 dB, four-pole Bessel filter), and sampling at 10 kHz. Recordings were digitized with a Digidata 1322A interface, driven by CLAMPEX 10 (Axon Instruments). Patch pipettes were made from borosilicate glass (2.0 mm O.D., WPI) and double pulled (Narishige PP-83) to resistances ranging from 2 to 5 MΩ when filled with the internal solution. For K_V channel recordings, the composition of this solution was (in mM): 125 KCl, 4 $MgCl_2$, 10 HEPES, 10 EGTA, 5 Mg^{2+}-ATP, pH 7.2 with KOH. The composition of the bath solution was (in mM): 141 NaCl, 4.7 KCl, 1.2 $MgCl_2$, 1.8 $CaCl_2$, 10 glucose and 10 HEPES, pH 7.4 with NaOH. The voltage dependence of K^+ currents were obtained applying 200 ms pulses from a holding potential of −80 mV to voltages between −60 to +60 mV in 20 mV steps, at a frequency of 5 s. Whole-cell patch-clamp recordings of TRPM3 currents were carried out with solutions of the following composition (in mM): 141 NaCl, 1.8 $CaCl_2$, 1.2 $MgCl_2$, 5 CsCl, 10 glucose, 10 HEPES, 0.005 nicardipine, 0.1 DIDS and 0.1 niflumic acid (pH 7.4 with NaOH) for the extracellular solution and 10 CsCl, 110 Cs aspartate, 10 NaCl, 3.2 $CaCl_2$, 10 HEPES, 10 BAPTA, 2 Mg^{2+}-ATP (pH 7.2, adjusted with CsOH) and with an estimated free [Ca^{2+}] of 100 nM for the intracellular solution. To determine the effects of PS (10 μM and 30 μM), CIM0216 (2 μM) and Uridine-5′-triphosphate (UTP, 100 μM) currents were recorded upon stimulation with 1 s voltage ramps from −150 mV to +80 mV applied from a holding potential of −10 mV, at a frequency of 5 s. Electrophysiological data analyses were performed with the Clampfit subroutine of pCLAMP (Axon Instruments) and with Origin 7.5 (OriginLab Corp.).

2.6. Pressure myography experiments

Third order mesenteric arteries were dissected and mounted in a myograph (Danish Myo Technology 110P) that allowed controlling the luminal pressure while measuring external arterial diameter via digital video edge detection (CCD camera). Artery segments were cannulated between two borosilicate glass pipettes and fixed with nylon filaments at both ends. The artery segments were filled with physiological saline solution containing (mM): 120 NaCl, 2.5 $CaCl_2$, 1.17 $MgSO_4$, 5 KCl, 1.18 Na_2HPO_4, 25 $NaHCO_3$, 1 EDTA, 10 glucose (pH 7.4, adjusted with 5% CO_2–95% air, which was maintained throughout the duration of the experiment) and were pressurized to 70 mmHg and allowed to stabilize at 37 °C for at least 15 min before starting the measurements. Unless otherwise stated the artery segments were air-bubbled though the lumen to remove endothelial cells. Phenylephrine (10 μM) or noradrenaline (NA, 20 μM) was perfused to contract the arteries prior to the application of test compounds. PS and CIM were washed after their last application with physiological saline solution containing 10 μM phenylephrine. The data were analyzed using MyoView software. At the end of each experiment, we applied the L-type Ca^{2+} channel blocker nifepidine (10 μM) to determine the maximum arterial diameter. Nifedipine was previously reported as a TRPM3 agonist [21]. Thus, it could be argued that nifedipine-induced vasodilation may be partly mediated by TRPM3, making this compound unsuitable for the determination of the role of this channel. To test this, we compared the vasodilation elicited in the same artery by 10 μM nifedipine application and by perfusion with Ca^{2+}-free bath solution. We observed similar increase in the arterial diameter in both cases (Fig. S1). This demonstrates that 10 μM of nifedipine has the same effect than abrogating Ca^{2+} entry through L-type Ca^{2+} channels, thus validating its use to determine the maximal vasodilation. Vasodilation was determined using the formula 100 x (Dx - DPhe)/(DNif - DPhe). Dx, DPhe and DNif were the diameters recorded in the presence of PS and phenylephrine, phenylephrine alone and nifedipine, respectively. The resulting dose-response curves for PS were fitted using either one or two Hill functions of the forms:

$$Vasodilation\ (in\%) = 100\frac{[PS]^n}{[PS]^n + k^n}$$

were *[PS]*, *n* and *k* are the PS concentration, the Hill coefficient and the effective concentration, respectively, and:

$$Vasodilation\ (in\%) = 100\left(\frac{A_1\,[PS]^{n1}}{[PS]^{n1} + k_1^{n1}} + \frac{(1 - A_1)[PS]^{n2}}{[PS]^{n2} + k_2^{n2}}\right)$$

where A_1, $n1$ and k_1 are the relative amplitude, the Hill coefficient and the effective concentration of the first Hill component, respectively, and $n2$ and k_2 are the Hill coefficient and the effective concentration of the second Hill component, respectively. A maximum of two arteries was taken from each mouse. In those cases, the data was averaged.

2.7. Intracellular Ca^{2+} imaging

Ca^{2+} imaging experiments were conducted using the fluorescent indicator Fura-2 AM. HEK293T cells stably expressing murine TRPM3 were cultured as previously described [19]. They were incubated with 5 μM Fura-2 AM (Invitrogen) for 30 min at 37 °C. Fluorescence measurements were performed with a Zeiss Axioskop FS upright microscope fitted with an ORCA ER charge-coupled device camera. Fura-2 AM was excited at 340 and 380 nm with a rapid switching monochromator (TILL Photonics). Mean fluorescence intensity ratios (F340/F380) were displayed online with Metafluor software (Molecular Devices).

2.8. Reagents

Pregnenolone sulfate, noradrenaline, propranolol and nifedipine were purchased from Sigma-Aldrich. CIM0216 was obtained from Prof. Joris Vriens. The CGRP receptor antagonist BIBN 4096 was obtained from Tocris Bioscience. K_V channel toxin blockers were purchased from Alomone Laboratories, and correolide was a gift from María García.

2.9. Statistical analyses

In all experiments, data were pooled from multiple trials carried out on cells or arteries isolated from at least three different animals and summarized as means ± SEM. The Origin software (version 8.6, OriginLab) was used for statistical analysis and data display. Differences between means were assessed using *t*-test paired or unpaired and one-way ANOVA, Dunn-Sidak test comparisons. $P < 0.05$ was taken as statistically significant difference between means.

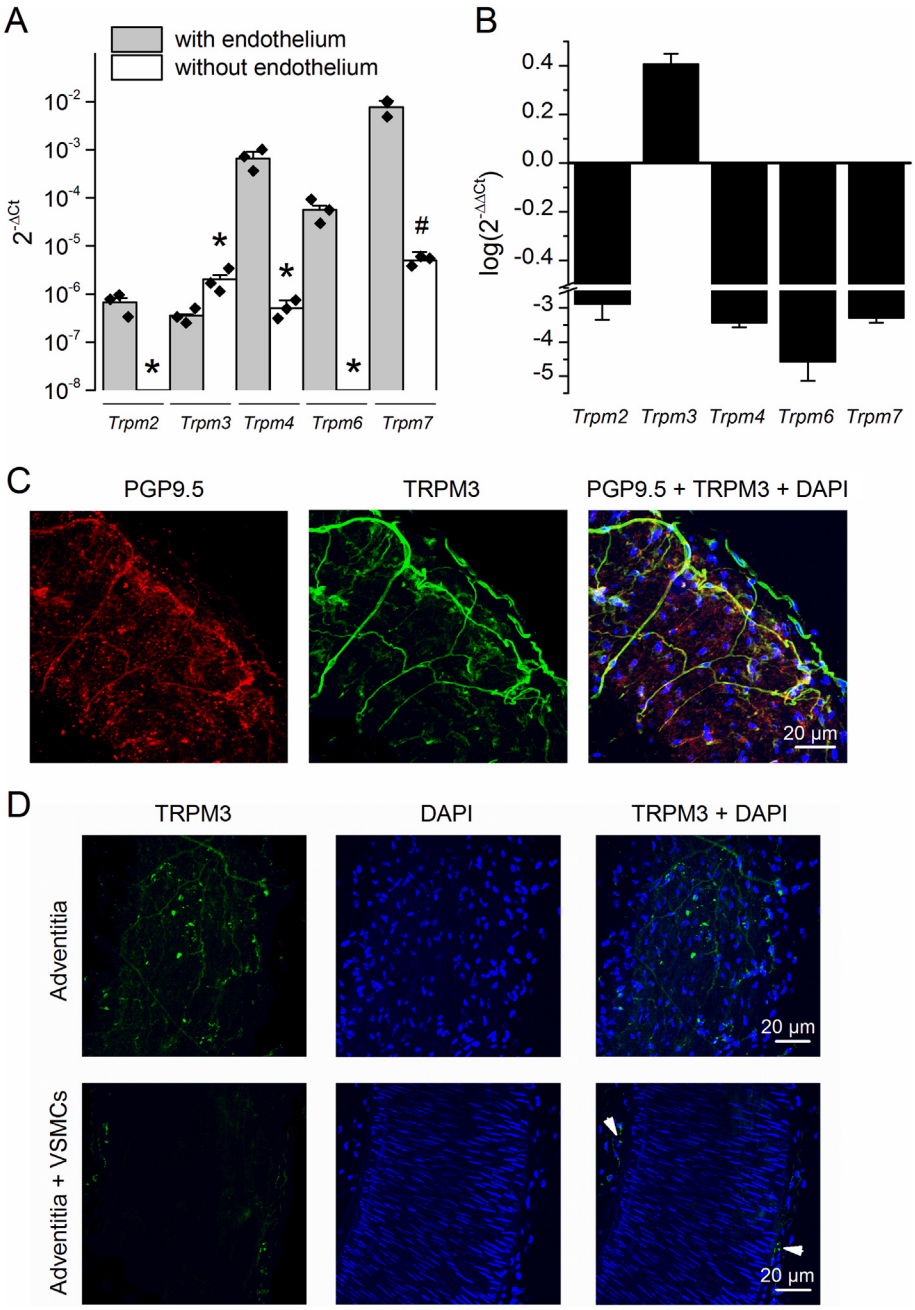

Fig. 1. TRPM3 is located in perivascular nerve endings of mouse mesenteric arteries. (A) Relative expression of *Trpm* genes in mesenteric arteries dissected from WT mice. Data are represented as mean ± SEM, *P < 0.05; #P < 0.01 (n = 3), one way ANOVA, Dunn-Sidak test. (B) Relative expression of *Trpm* genes in endothelium-denuded arteries using arteries with endothelium as calibrator. Data are mean ± SEM (n = 3 different pools of arteries from 5 different mice). (C) Confocal images of intact WT mouse mesenteric arteries labeled with PGP9.5 (left) and TRPM3 (center) antibodies. An overlay of these images merged with a nuclear staining DAPI (blue) is shown on the right. (D) Confocal microscopy images of the adventitia and medial layers labeled with a TRPM3 antibody (green) and nuclear DAPI staining (blue). The white arrowheads in the bottom-right image point to TRPM3 labeling observed only in the adventitial layer. Images are representative of at least 3 independent samples. (For interpretation of the references to colour in this figure legend, the reader is referred to the web version of this article.)

3. Results

3.1. Expression pattern of TRPM family in mouse mesenteric arteries

We first determined the expression of the genes encoding TRPM channels in WT mouse mesenteric arteries with and without endothelium. *Trpm1*, *Trpm5* and *Trpm8* could not be detected after 40 cycles of amplification in any preparation. In contrast, the other 5 members of the subfamily were detected in preparations with endothelium (Fig. 1A). We found lower relative expression for *Trpm4* and *Trpm7* and no detectable *Trpm2* and *Trpm6* in preparations devoid of endothelium (Fig. 1A, B), suggesting for a preferential expression of these transcripts in the endothelial layer. In sharp contrast, we found higher relative levels of *Trpm3* mRNA in endothelium-free preparations, indicating for a predominant expression in the medial and/or adventitial layers. Of note, we found a much higher relative abundance of *Trpm3* mRNA in aorta than in mesenteric arteries (3.3 ± 0.8; n = 3 versus 0.09 ± 0.01; n = 3; P < 0.001; data not shown).

3.2. Localization of TRPM3 in perivascular nerves of mouse mesenteric arteries

Confocal images of mesenteric arteries labeled with the neuronal markers PGP9.5 (Fig. 1C) and neurofilament (NF-200; Fig. S2A) evidenced the presence of nerve fibers in the adventitial layer, but not deep in the smooth muscle layer (Fig. S2B). The localization of TRPM3 was determined with an antibody whose specificity against TRPM3 was confirmed in a HEK293T cell line stably transfected with this channel (Fig. S3). As control for the experiment, we used TRPM5-transfected HEK293T cells, which also express TRPM7 endogenously [22]. We found that these cells were not stained with the anti-TRPM3 antibody, confirming the specificity for TRPM3 versus these closely-related TRPM channels (Fig. S3). We found that TRPM3 colocalized with PGP9.5 (Fig. 1C) and was absent in cells of the tunica media (VSMC), which

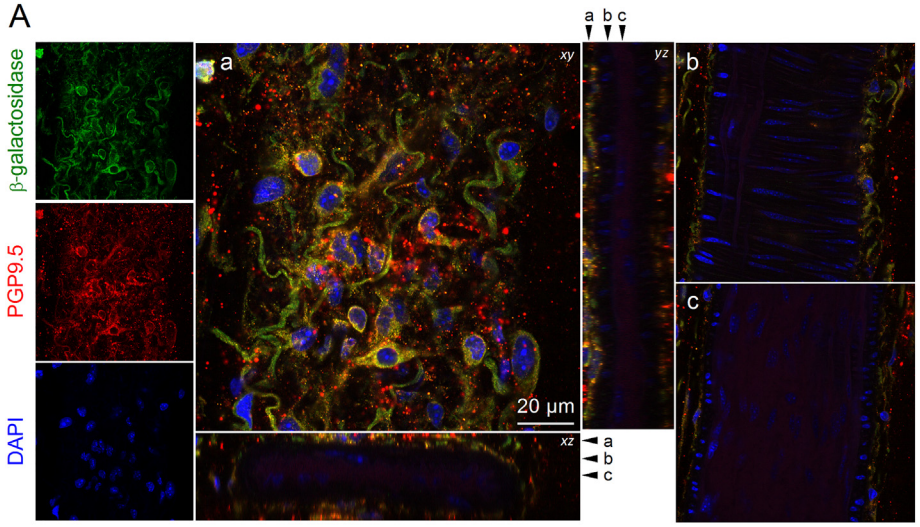

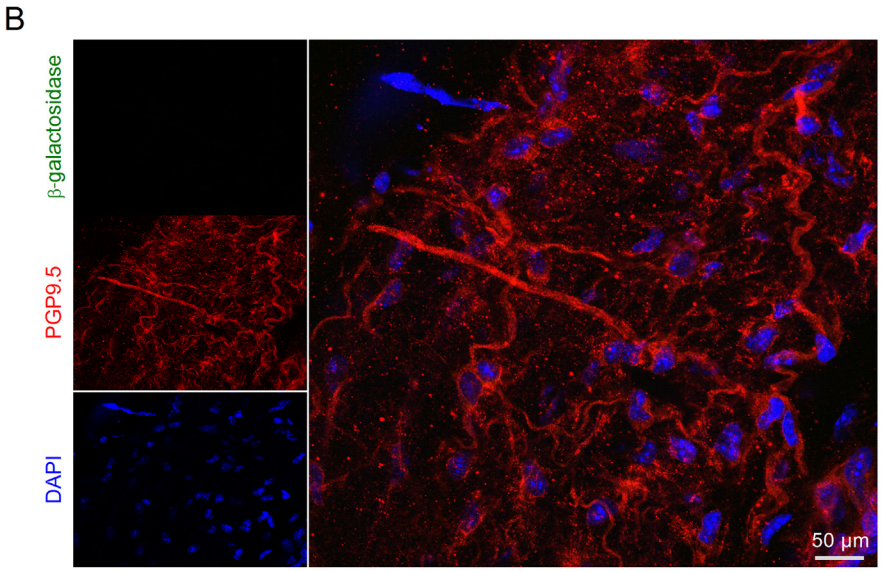

Fig. 2. Location of the transgene product of the *Trpm3* KO mice in perivascular nerve endings of mesenteric arteries. (A) *Z*-stack confocal images of intact *Trpm3* KO mouse mesenteric arteries at the levels of the adventitial (a), medial (b) and endothelial (c) layers, labeled with β-galactosidase (green), PGP9.5 (red) antibodies and nuclear DAPI (blue) staining. The images are representative of at least 3 independent samples. (B) Confocal microscopy images of the adventitial layer of a WT mouse mesenteric artery labeled with β-galactosidase (green), PGP9.5 (red) antibodies and nuclear DAPI staining (blue). Images are representative of at least 3 independent samples. (For interpretation of the references to colour in this figure legend, the reader is referred to the web version of this article.)

were clearly identified by the distinct orientation of their nuclei, perpendicular to the axis of the vessel (Fig. 1D).

Of note, arteries from *Trpm3* KO mice could not be used as a negative control for the TRPM3 antibody, because these animals express a truncated TRPM3 protein that can be recognized by the anti-TRPM3 antibody. However, we took advantage of the fact that these mice have incorporated a β-galactosidase (β-gal) reporter encoded by the insertion of a *Lac-Z* gene into the reading frame of the *Trpm3* gene [20]. Using an anti-β-gal antibody in *Trpm3* KO mice, we found that β-gal colocalized with the neuronal markers PGP9.5 (Fig. 2A) and NF-200 (Fig. S2A) and was absent in VSMC (Fig. S2B). As expected for negative control, WT arteries were not stained with the anti-β-gal antibody (Fig. 2B). To further characterize the localization pattern of TRPM3 we performed double immunostaining in intact mesenteric arteries from *Trpm3* KO mice labeled with antibodies against β-gal and the smooth muscle-specific protein alpha-smooth muscle actin (α-SMA). We found α-SMA to be present as expected in the smooth muscle (Fig. 3A), but not in the adventitial layer (Fig. 3B). In contrast, β-gal was clearly detected only in nerve ending-like structures in the adventitial layer.

To test directly whether TRPM3 is functionally expressed in the medial layer of mouse mesenteric arteries we performed whole-cell patch-clamp recordings in freshly dissociated VSMC. Application of PS (10 and 30 μM) produced no significant change in the current amplitude at −80 mV and + 150 mV (99.9 ± 0.5% and 100 ± 0.3% relative to the amplitude recorded in control condition, respectively; n = 12 cells from 4 mice; Fig. 4A). In another series of experiments, the effects of PS (10 μM) and of the potent TRPM3 synthetic agonist CIM0216 [18] on current amplitude were compared to the effects of the purinergic receptor agonist UTP [23]. Again, there was no change in current amplitude during PS application (−0.3 ± 0.3 pA, P = 0.95, at −150 mV and 1.3 ± 0.9 pA, P = 0.77 at +80 mV) (n = 6 cells from 3 mice; Fig. 4B, black trace in right panel). Currents were also unaffected by 2 μM CIM0216 (current amplitude change of −0.5 ± 1.7 pA, P = 0.99 at −150 mV and 2 ± 2 pA, P = 0.77 at +80 mV; n = 4 cells from 2 mice; Fig. 4C, black trace in right panel). On the other hand, currents were stimulated at negative potentials by 100 μM UTP, as expected. The amplitude of the UTP-sensitive current was −51 ± 9 pA, P = 0.003 at −150 mV and 2.7 ± 0.7 pA, P = 0.26 at +80 mV; n = 5 cells from 2 mice (Fig. 4B, C, grey traces in right panels). Taken together, these data indicate the absence of functional expression of TRPM3 channels in mesenteric arteries VSMCs.

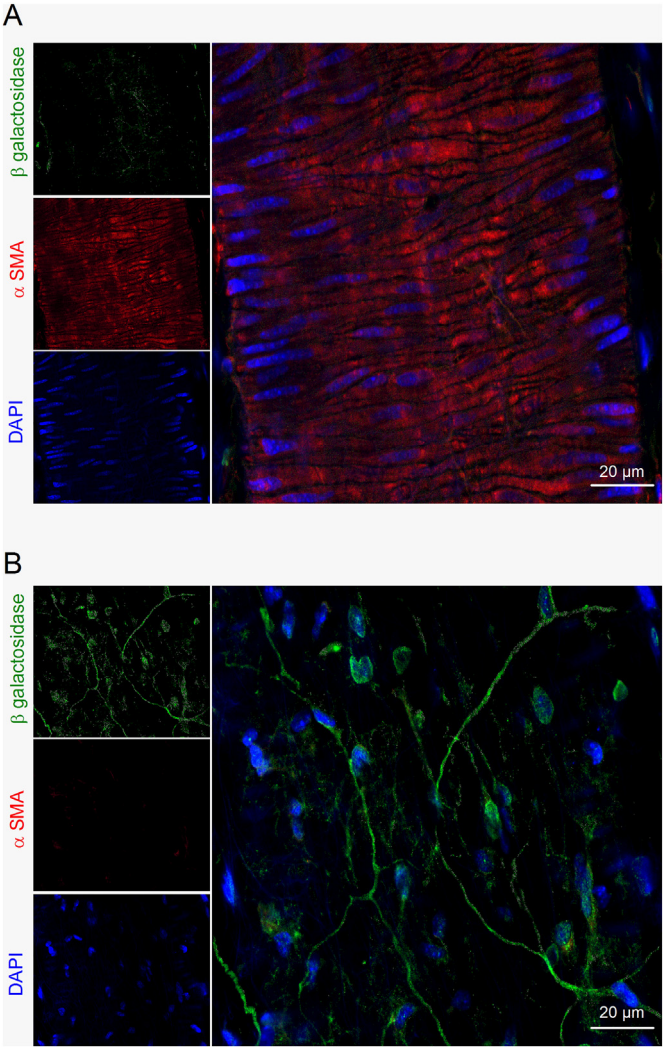

Fig. 3. The transgene product of the *Trpm3* KO mice is not located in smooth muscle layer from mesenteric arteries. Confocal microscopy images of the medial layer (A) and adventital layer (B) of *Trpm3* KO mouse intact mesenteric arteries labeled with β-galactosidase (green), α-smooth muscle actin (red) antibodies and nuclear DAPI staining (blue). Images are representative of at least 3 independent samples. (For interpretation of the references to colour in this figure legend, the reader is referred to the web version of this article.)

3.3. TRPM3 activation induces vasodilation via stimulation of CGRP receptors

To determine the effects of TRPM3 activation in resistance arteries we performed pressure myography experiments in endothelium-denuded mouse mesenteric arteries. Pressurized arteries were pre-contracted with 10 μM phenylephrine to maintain the physiological tone. PS induced a dose-dependent reversible vasodilation in arteries dissected from WT animals. The data was best fit by the sum of two Hill functions, suggesting for at least two targets of PS (Fig. 5A, D). The EC_{50} values for these components were 14 ± 2 μM and 100 ± 9 μM and the corresponding Hill coefficients (H) were 2.2 ± 0.5 and 4.3 ± 1.2, respectively. This fitting also yielded a value of relative amplitude of the low EC_{50} vasodilation component of 57 ± 7% (A_1, see the two-Hill components equation in the Methods, section Pressure myography experiments). To determine the contribution of TRPM3 channels to the effects of PS we measured the response of mesenteric arteries isolated from *Trpm3* KO mice. PS dilated *Trpm3* KO arteries only at concentrations higher than ~10 μM (Fig. 5B, D). The dose-response curve for *Trpm3* KO arteries could be fitted with a single Hill function, with EC_{50} and Hill values of 53 ± 3 μM and 2.2 ± 0.2, respectively. These results further support the idea that in WT arteries there are two different mechanisms involved in PS-induced vasodilation, being only the one with lower EC_{50} TRPM3-dependent. Also, CIM0216 induced a dose-dependent reversible vasodilation in arteries from WT animals, with EC_{50} and Hill coefficients values of 0.40 ± 0.05 μM and 0.65 ± 0.06, respectively (Fig. S4A, C). Arteries dissected from *Trpm3* KO mice responded to this compound, but at concentrations higher than 0.1 μM, with EC_{50} and Hill coefficients values of 1.50 ± 0.08 μM and 1.6 ± 0.1, respectively (Fig. S4B, C).

Based on prior studies on sensory TRP channels such as TRPV1 and TRPA1 [8,9] and the expression of TRPM3 in nociceptive neurons [18,19], we hypothesized that the TRPM3-dependent vasodilation induced by PS may be mediated by the release of CGRP and the relaxing effect of this peptide on VSMC. To test this, we performed myography experiments in the presence of the CGRP receptor antagonist BIBN 4096. In this condition, PS-induced vasodilation could only be elicited at concentrations above 10–15 μM (Fig. 5C). The dose-response curve of the effect of PS in the presence of BIBN 4096 was similar to the curve obtained in arteries from *Trpm3* KO mice, with EC_{50} and H values of 44 ± 2 μM and 1.8 ± 0.1, respectively (Fig. 5D). Furthermore, double immunolabelling of intact mesenteric arteries from *Trpm3* KO mice with anti-β-gal and anti-CGRP antibodies showed a good colocalization in the sensory fibers (Fig. 5E). These results indicate that TRPM3 location seems to be restricted to sensory nerve endings, where the TRPM3-mediated effect of PS depends on CGRP receptor activation.

The vasodilating action of CGRP has endothelium-dependent and endothelium-independent components, which are mediated by the stimulation of CGRP receptors in endothelial cells and VSMC, respectively [24,25]. Thus, the TRPM3-dependent effect of PS is expected to be stronger in the presence of endothelium. We found that this was indeed the case, as PS induced a dose-dependent biphasic effect in intact arteries (Fig. S5A), with EC_{50} values lower than the corresponding ones found in endothelium-denuded preparations (8.1 ± 0.5 μM and 50 ± 2 μM) (Fig. S5B).

3.4. CGRP release induces vasodilation via activation of K^+ channels

Next, we explored the mechanisms by which CGRP receptor activation in VSMC leads to vasodilation. Stimulation of the CGRP receptor has been reported to increase cyclic adenosine monophosphate (cAMP) production via the adenylate cyclase (AC) [26] and may therefore lead to protein kinase A (PKA)-mediated activation of K^+ channels in VSMC and consequent hyperpolarization and arterial relaxation. To test whether activation of K^+ channels is involved in the vasodilation response triggered by TRPM3 activation we compared the effects of 10 μM PS in arteries treated or not with K^+ channel blockers. We noticed that the vasodilation induced by acute application of 10 μM PS (42 ± 4%, n = 14) in the presence of phenylephrine (10 μM) (Fig. 6A) was larger than that induced by the same concentration during the cumulative dose-response experiments (18 ± 4%, n = 10). This may be due to partial CGRP depletion induced by previous applications of PS at low concentrations. Nevertheless, the effects of cumulative (Fig. 5D) or acute (Fig. S6) application of 10 μM PS were largely mediated by CGRP. Pretreatment with the voltage- and Ca^{2+}-activated K^+ channel blocker paxilline (500 nM) [27] and the K_V1 channels blocker correolide (10 μM) [28] led to a significant reduction of the effect of PS on pre-contracted mesenteric arteries. This effect was enhanced by addition of the K_V2 blocker stromatoxin (ScTx1, 50 nM) (Fig. 6A, B) [29]. None of these compounds affected the responses of HEK293T cells stably transfected with mouse TRPM3 to PS (Fig. S7A), indicating that they did not target TRPM3 in the arterial preparations. We also probed for direct modulatory effects of PS on K_V channels in whole-cell patch-clamp experiments performed in mesenteric VSMC freshly isolated from WT and *Trpm3* KO mice. Current-voltage relationships elicited in WT and in *Trpm3* KO VSMC by depolarizing pulses were unaffected by

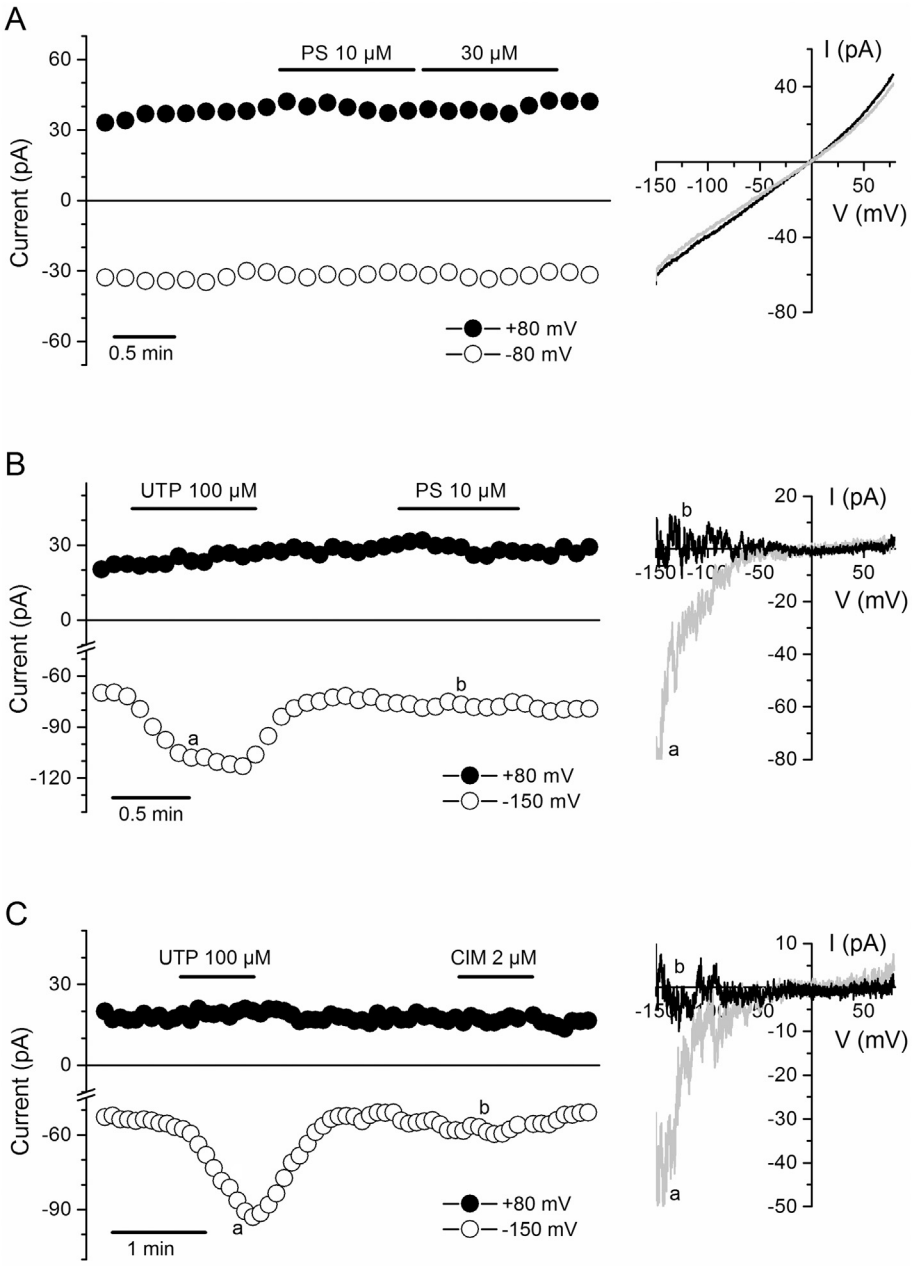

Fig. 4. TRPM3 is not functionally expressed in WT mouse mesenteric VSMC. (A) Left, time course of the amplitude of currents recorded at −80 and + 80 mV in control and in the presence of 10 and 30 µM PS. Right, average of current traces recorded in control (black) and in the presence of 30 µM PS (grey). (B, C) Left, representative examples of the time course of the amplitude of currents recorded at −150 and + 80 mV, showing the effects of 100 µM UTP, 10 µM PS and 2 µM CIM0216. Right, the traces represent the differences between traces recorded in the presence of these compounds at the time points indicated by the labels a and b and a corresponding current trace recorded in control.

application of PS (10 and 30 µM; Fig. S7B, C).

We further assessed the implication of the cAMP pathway and K^+ channels by testing the effects of forskolin, a direct activator of AC, both in the absence and in the presence of paxilline, correolide and stromatoxin. We found 1 µM forskolin to induce strong vasodilation, an effect that was significantly attenuated in the presence of the K^+ channel blockers (Fig. 6C, D). Taken together, these results indicate that the TRPM3-mediated dilation of mesenteric arteries is at least partly mediated by the activation of K_V channels in VSMC.

3.5. Sympathetic nerves are not implicated in TRPM3-mediated vasodilation

The tone of mesenteric arteries is regulated by sympathetic innervation through the release of noradrenaline. The dominant effect of noradrenaline on mesenteric arteries is α_1-adrenoreceptor-mediated vasoconstriction, but mesenteric VSMC also express β_2-adrenoreceptors, whose activation could induce vasodilation. If TRPM3 channels were also expressed in sympathetic nerve endings, PS-induced dilation of mesenteric arteries could be partly mediated by the activation of β_2-adrenoreceptors. We used several approaches to assess this possibility. First, we studied the functional contribution of β_2-adrenoreceptors to the sympathetic response. The application of 20 µM noradrenaline led to a vasoconstriction that was not affected by the application of the selective β_2-antagonist propranolol (1 µM and 5 µM; Fig. 7A). This suggests that the effects of sympathetic stimulation on mesenteric vessels are exclusively mediated by noradrenaline acting on α_1-adrenoreceptors. Consistently with this, we failed to find any vasodilation in response to noradrenaline application in Phe-pre-contracted arteries (Fig. 7B). In another series of experiments, we found that PS (10 µM) induced vasodilation in the presence of 5 µM propranolol (Fig. 7C, 40.3 ± 1.2 µM, n = 3), further indicating that β_2-adrenoreceptors are not involved in the vasodilation induced by PS. In addition, we performed double immunostainings of intact mesenteric arteries of *Trpm3* KO mice using anti-β-gal and anti-Tyrosine hydroxylase (TH) antibodies. We found β-gal-positive structures in the adventitia that

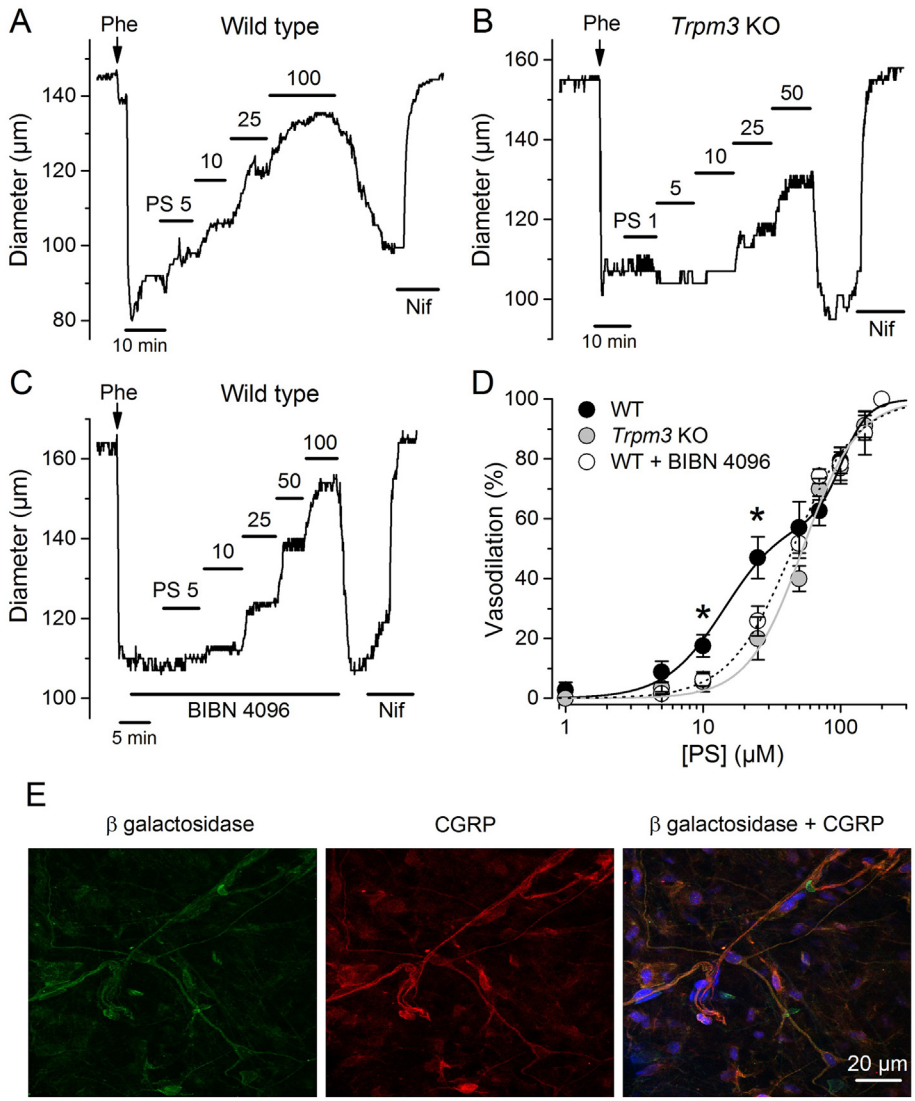

Fig. 5. TRPM3-induced vasodilation of mesenteric arteries is mediated by CGRP receptor activation. Representative examples of the effects of increasing concentrations of pregnenolone sulfate (PS, in μM) on the diameter of arteries dissected from WT (A) and *Trpm3* KO mice (B) in the presence of phenylephrine (Phe, 10 μM). (C) Effects of PS (in μM) on WT arteries in the presence of the CGRP receptor antagonist BIBN 4096 (1 μM) and phenylephrine (10 μM). Nifedipine (Nif, 10 μM) was applied at the end of each experiment. (D) Dose dependency of PS-induced vasodilation (in μM) in precontracted arteries dissected from WT, *Trpm3* KO mice and in WT arteries in the presence of 1 μM BIBN 4096. Data are mean ± SEM (n = 10 arteries from 8 WT mice; n = 8 arteries from 7 *Trpm3* KO mice and n = 8 arteries from 6 WT animals + BIBN 4096). The black solid line represents the fit of the WT data with a two-component Hill equation. The grey solid line and the dotted line represent the fit of the data for *Trpm3* KO and WT in the presence of BIBN 4096 with single-component Hill equations. * indicates $P < 0.05$ compared to WT mice, unpaired *t*-test. (E) Confocal images of intact *Trpm3* KO mouse mesenteric arteries of the adventitial layer labeled with β-galactosidase (green), CGRP (red) antibodies and nuclear DAPI staining (blue). Images are representative of at least 3 independent samples. (For interpretation of the references to colour in this figure legend, the reader is referred to the web version of this article.)

were clearly not stained for TH (Fig. 8, white arrow heads in the bottom-left panel). We did observe some overlap between β-gal- and TH-positive structures, but it seems that this was due to their close proximity and not to an actual co-expression of β-gal and TH in the same nerve endings (Fig. 8, adventitia, left panels). The reason for this is that the β-gal labeling, but not the TH one, was progressively lost as the images were taken closer to the medial layer (Fig. 8, advent. + VSMC, right panels). Note that it seems highly unlikely that β-gal and TH would localize in the same fibers and that only the expression of the former, being an exogenous and probably unregulated protein, suddenly stops at the points of fibers entry into the medial layer. Altogether, our functional and anatomical experiments point to a lack of involvement of sympathetic fibers in TRPM3-mediated vasodilation.

4. Discussion

TRP channels have been found in all cell types relevant for vascular function. Endothelial TRP channels regulate angiogenesis and vascular tone and permeability, whereas in VSMC they are implicated in the regulation of contraction and proliferation [2,30]. TRP channels are also expressed in perivascular cells, such as TRPV4 in astrocytes and TRPV1 and TRPA1 in sensory neurons [2]. Here we investigated the expression and function a TRP channel of emerging relevance, TRPM3, in resistance arteries.

Although we found *Trpm3* mRNA in VSMC and adventitia layer (Fig. 1A, B), our anatomical and functional data are consistent with an expression of TRPM3 protein restricted to perivascular nerve endings (Figs. 1C and D, 2, 3, 4, 5E, 7 and S2). A previous report showed functional expression of TRPM3 channels in proliferating human VSMC and in freshly isolated mouse aortic myocytes [17], but we did not find responses to PS in freshly isolated mouse mesenteric myocytes (Fig. 4A, B). Whether these differences may reflect vascular bed-dependent functional expression of TRPM3 requires further investigation. Our qPCR studies show that *Trpm3* mRNA expression is almost 40 times higher in aorta than in mesenteric arteries (data not shown). This is in line with TRPM3 channels being functionally expressed in aortic VSMC, activation of which leads to Ca^{2+} entry and vasoconstriction [17].

In contrast to these previous observations in aorta [17], we found that PS induces vasodilation of mesenteric arteries (Fig. 5A). The maximal effect of this compound was comparable to the maximal dilation induced by nifedipine or a Ca^{2+} free solution (Fig. S1). A previous report showed that genetic ablation of *Trpm3* abolished CGRP release from skin and insulin secretion from isolated pancreatic islets in response to 100 μM PS [18]. However, we found that PS induced dilation via two components, being the high EC_{50} component still present in arteries isolated from *Trpm3* KO mice (Fig. 5B, D). Our results show that PS has TRPM3-independent effects in mesenteric arteries at concentrations higher than 10 μM. This compound has been shown to act

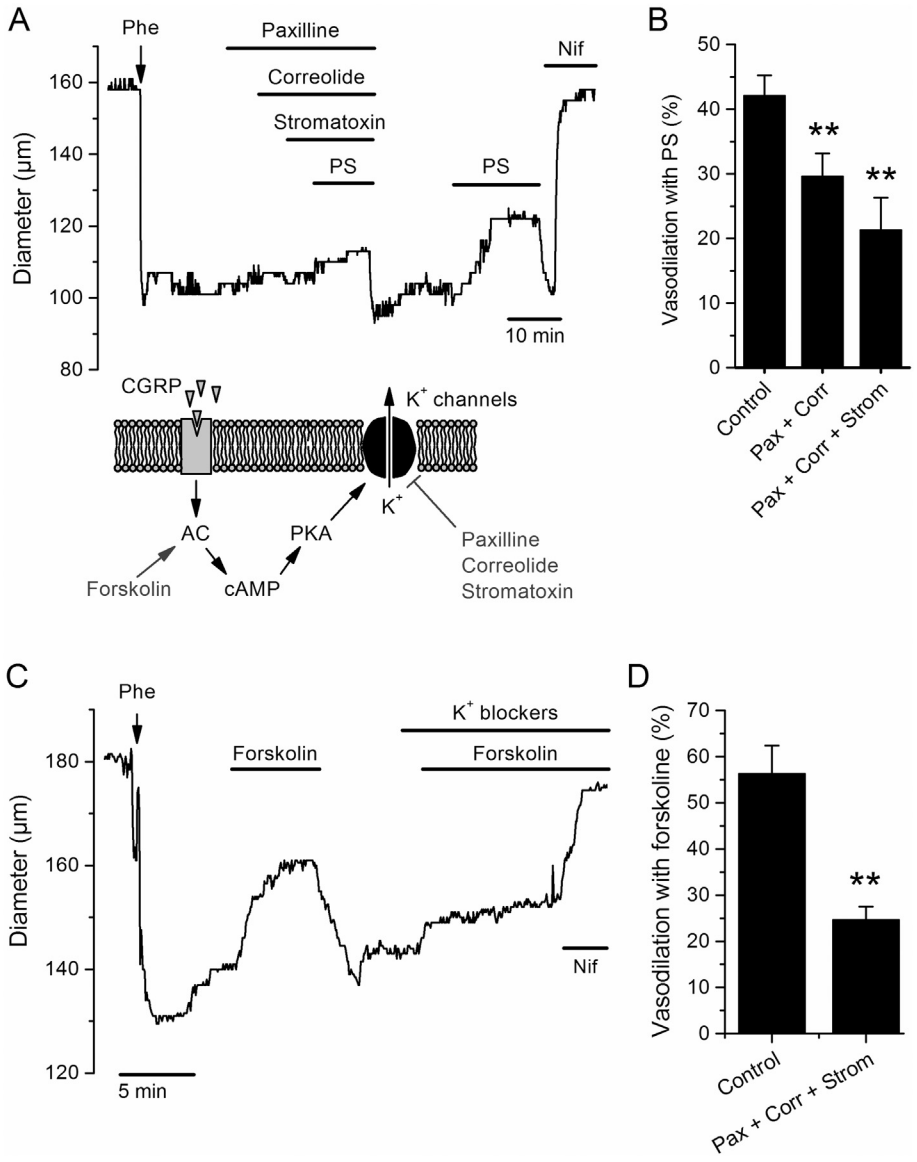

Fig. 6. TRPM3-dependent vasodilation is partly mediated by activation of K^+ channels and further stimulation of adenylate cyclase. (A) Comparison of the effects of pregnenolone sulfate (PS, 10 µM) in control conditions and in the presence of the K^+ channel blockers paxilline (500 nM), correolide (10 µM) and stromatoxin (50 nM). The scheme shows the CGRP signaling cascade leading to activation of K^+ channels via stimulation of adenylate cyclase (AC) and protein kinase A (PKA) in VSMC. (B) Average vasodilator effects of 10 µM PS on WT mesenteric arteries in control conditions (n = 14 arteries from 10 mice), in the presence of paxilline and correolide (n = 8 arteries from 5 mice) and in the presence of paxilline, correolide and stromatoxin (n = 5 arteries from 4 mice). * indicate $P < 0.05$ for the comparison with the data obtained in control, unpaired t-test. (C) Representative example of the effect of 1 µM forskolin on a WT mouse mesentery artery in control and in the presence of the K^+ channel blockers paxilline (500 nM), correolide (10 µM) and stromatoxin (50 nM). (D) Average vasodilator effect of 1 µM forskolin in the absence (n = 4 arteries from 4 mice) and in the presence of K^+ channel blockers (n = 4 arteries from 4 mice). Phe = Phenylephrine; Nif = nifedipine * indicates $P < 0.05$ versus control, paired t-test.

on other targets, such as the gamma-aminobutyric acid receptor A and the *N*-methyl-D-aspartate receptor [31], but it is not yet clear whether these bare any relevance in mesenteric arteries. Of note, the values of the EC_{50} and Hill coefficient corresponding to the TRPM3-independent PS responses were different in WT and *Trpm3* KO arteries. This may be due to the fact that in WT arteries the TRPM3-dependent processes may affect the TRPM3-independent vasodilation observed at higher PS concentrations. The nonlinear and integrative character of the vasodilation process may preclude that the effects of individual PS-dependent components add up in a simple arithmetic way. Further assessment of this observation will be possible once the mechanism underlying the latter component is clarified. Nevertheless, the data fitting results indicate that the TRPM3-dependent component contributes to an important fraction of the total PS-induced dilation of WT arteries (~60%), and its occurrence in the lower concentration range suggest that it is the most relevant component in physiological conditions.

In regard to the mechanism underlying TRPM3-dependent vasodilation, the overlap we observed between the PS dose response curves obtained for *Trpm3* KO arteries and for WT arteries in the presence of the CGRP receptor inhibitor suggests that PS-induced CGRP effects are fully mediated by TRPM3 (Fig. 5D). Previous studies demonstrated CGRP release upon TRP channel activation in mouse trachea [32] and hind paw skin [18]. However, we were unable to detect CGRP release from mesenteric using similar experimental procedures (data not shown), most likely because our preparation is between ~200- and 2000-fold smaller than the trachea and skin ones, respectively.

The mechanisms proposed for the vasodilating effects of CGRP include an endothelium-dependent component, whereby activation of the endothelial CGRP receptor results in a rise in cAMP, NO production and guanylate cyclase-mediated vasodilation [33]. In addition, there are two effects mediated by AC and PKA stimulation in VSMC: activation of K^+ channels and stimulation of myosin light chain phosphatase [24,34]. Our data are consistent with all these mechanisms, as we found that the responses to PS were enhanced in the presence of endothelium and were partially inhibited by a cocktail of K^+ channel blockers (Fig. S5 and 6A, respectively). Furthermore, we could exclude a possible contribution of sympathetic fibers to the PS-induced vasodilation mechanisms. Our data discard both the functional contribution of β_2-adrenoreceptors to the sympathetic response and the involvement of these receptors in the vasodilation induced by PS application, as no differences were observed when we applied the β-blocker propranolol (Fig. 7). Moreover, as explained in the Results, the absence of colocalization of TH and β-gal in the nerve fibers innervating the medial layer (Fig. 8) indicates a lack of expression of TRPM3 in sympathetic nerve

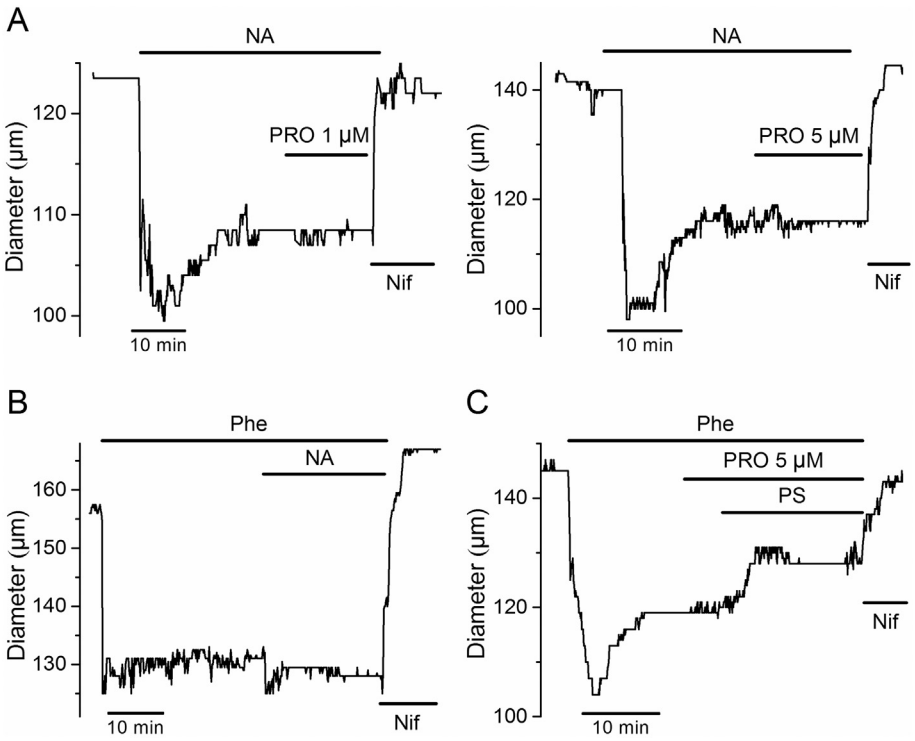

Fig. 7. Sympathetic perivascular nerves are not involved in TRPM3-induced vasodilation of mesenteric arteries. (A) Representative example of the effect of noradrenaline (NA, 20 µM) on a WT mouse mesentery artery in the presence of the β-adrenoreceptor blocker propranolol (PRO, 1 µM in the left panel and 5 µM in the right panel). (B) Effect of 10 µM noradrenaline on WT arteries precontracted with phenylephrine (Phe, 20 µM). (C) Effect of pregnenolone sulfate (PS, 10 µM) in the presence of propranolol (5 µM). Nifedipine (Nif, 10 µM) was applied at the end of each experiment.

endings. Notably, it was previously shown that CGRP-containing fibers and TH-containing fibers can be found in close proximity of each other in mouse mesenteric arteries, and that the former run further away from the VSMC [35], as we found for TRPM3- and β-gal-expressing nerves (Figs. 1, 2, 3 and 8).

Notably, the vasodilation we report here is the most sensitive TRPM3-mediated tissue response to PS reported so far. Previous studies showed TRPM3-dependent effects of PS in the range of tens to hundreds of micromolar, e.g., insulin release from pancreatic islets [21], CGRP release form mouse skin preparations [18] and rat ductus arteriousus contraction [36]. In contrast, we found significant TRPM3-dependent vasodilation with an EC_{50} of 7.7 µM in intact arteries. This value is the most similar to those reported for stimulation of TRPM3 currents in vitro (5–23 µM) [37,38]. Most likely, this is a consequence of the technical approach in myography experiments since PS has direct access to the TRPM3-expressing nerve endings, which contrasts with other preparations in which structural barriers are expected to interfere with PS diffusion. This suggests the mesenteric artery preparation as very instrumental for studies on TRPM3 modulation and pharmacology, including the testing of the specificity of previously described channel inhibitors [39,40], in a close-to-physiological context. In addition, our results shed light on the long-standing question of whether PS is after all a physiological endogenous agonist of TRPM3 [21]. We observed TRPM3-dependent vasodilation induced by PS in the low micromolar range (Fig. 5A), which matches PS concentrations that may be present in living tissues [21]. The physiological or pathological contexts in which PS reaches such concentrations in mesenteric tissue remain, however, elusive. The idea that TRPM3 activation induces vasodilation in mesenteric arteries is further supported by the potent effect of the synthetic agonist CIM0216. However, this compound proved not to be fully specific for this channel, as it also produced vasodilation in arteries dissected from *Trpm3* KO mice at concentrations above ~0.1 µM (Fig. S4). We argue, therefore, that CIM0216 may be used as pharmacological tool to further investigate the role of TRPM3 in mesenteric arteries below these concentrations. Because this is a synthetic compound with no obvious similarity to any other known TRPM3 modulator [18], we consider that investigating the TRPM3-independent effects is interesting but beyond the scope of the present study. Nevertheless, reporting for the first time that CIM0216 has off-target effects is of great value for future research on TRPM3 pathophysiology.

The functional expression of TRPM3 in nociceptive neurons and its contribution to noxious heat sensing [19] may suggest that the function of this channel in mesenteric arteries is the detection of noxious stimuli generated in pathological conditions. The high temperatures required for TRPM3 activation [19] strongly indicate that heat may not be a relevant stimulus of TRPM3 in mesenteric preparations. Nevertheless, it would be interesting to determine whether this channel is implicated in responses of skin resistance arteries to heat. However, in contrast to previous reports in skin and trachea [18,19], we show here for the first time a role of TRPM3 in sensory fibers innervating a tissue that is not directly accessible to external stimuli. This may indicate that TRPM3 functions as detector of endogenous compounds released upon tissue damage and/or metabolic deregulation. Two other sensory TRP channels, TRPV1 and TRPA1 are proposed to act as receptors of danger- and pathogen-associated molecular patterns during tissue injury and inflammatory diseases [41], by detecting acidosis, reactive oxygen and nitrogen species, electrophilic compounds and bacterial endotoxins [2,8,32,42–45]. However, TRPV1 and TRPA1 have also been reported in VSMC and endothelial cells of resistance arteries, respectively [46–50]. Thus, according to our findings, TRPM3 is the only one of these sensory TRP channels exclusively functional in perivascular nerves. This suggests TRPM3 as the most specific target to trigger resistance artery vasodilation via stimulation of the perivascular sensory innervation.

We conclude that in contrast to what was previously reported in aorta [17], in mesenteric arteries TRPM3 is functionally expressed mainly in perivascular nerve endings and its activation leads to vasodilation rather than contraction. Our data is consistent with a model in which activation of TRPM3 triggers CGRP release, leading to vasodilation via endothelium-dependent and endothelium-independent pathways. We propose that, together with TRPV1 and TRPA1, TRPM3 allows mesenteric arteries to react to a wide range of damage-associated molecules, leading to vasodilation, via the common pathway of CGRP release from perivascular sensory nerve endings.

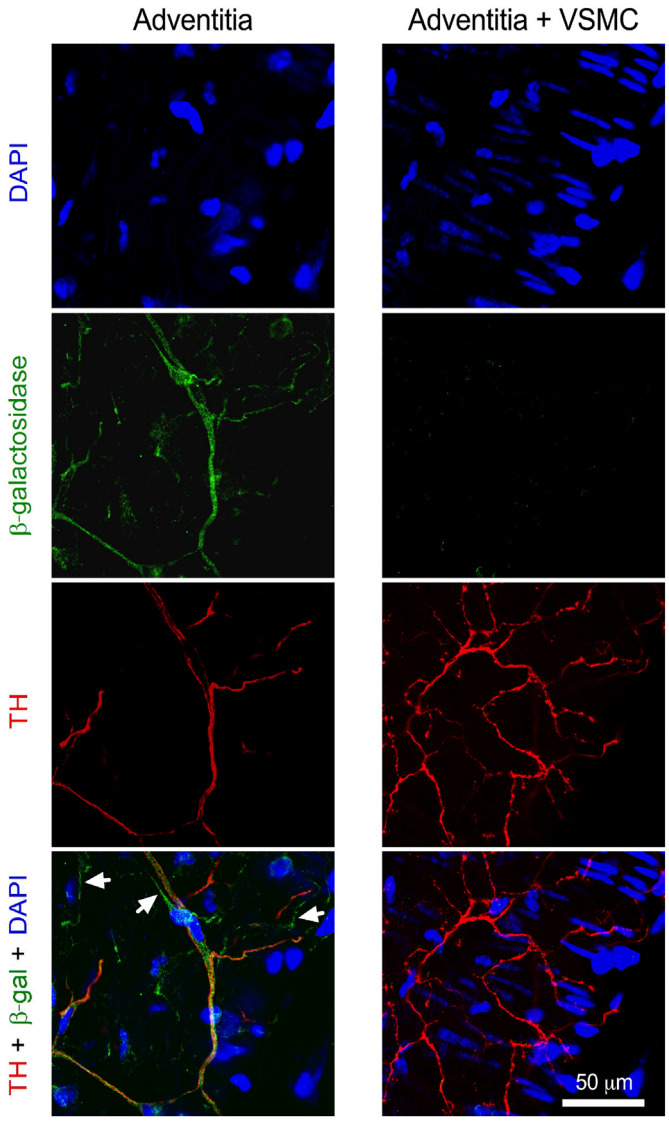

Fig. 8. Comparison of the location of the transgene product of the *Trpm3* KO mice (β-galactosidase) with that of adrenergic (Tyrosine hydroxylase-labeled) nerve fibers. Confocal images of an intact *Trpm3* KO mouse mesenteric artery taken at the level of the adventitial (left panels) or closer to the medial (right panels) layers, labeled with nuclear DAPI staining (blue), β-galactosidase (green, β-gal) and Tyrosine hydroxylase (red, TH). Images are representative of at least 3 independent arterial samples. The arrowheads in the left-bottom panel indicate β-gal-labeled structures not stained for TH. (For interpretation of the references to colour in this figure legend, the reader is referred to the web version of this article.)

Funding

This work was supported by grants from the Fund for Scientific Research Flanders (FWO, G.0C68.15, Belgium) to KT, the Ministerio de Economía y Competitividad (BFU2013-45867-R and BFU2016-75360-R, Spain) to JRLL and MTPG and Junta de Castilla y León(VA114P17, Spain) to MTPG. Y.A.A. is a Postdoctoral Fellow of the FWO (Belgium).

Disclosures

None.

Acknowledgments

We thank the members of the Laboratory of Ion Channel Research for helpful discussions and specially Prof. J. Vriens for providing the TRPM3 agonist CIM0216. We also thank T. Arranz and E. Alonso for excellent technical assistance.

Appendix A. Supplementary data

Supplementary data to this article can be found online at https://doi.org/10.1016/j.yjmcc.2019.03.003.

References

[1] L. Alonso-Carbajo, M. Kecskes, G. Jacobs, A. Pironet, N. Syam, K. Talavera, R. Vennekens, Muscling in on TRP channels in vascular smooth muscle cells and cardiomyocytes, Cell Calcium 66 (2017) 48–61.
[2] S. Earley, J.E. Brayden, Transient receptor potential channels in the vasculature, Physiol. Rev. 95 (2) (2015) 645–690.
[3] G. Owsianik, K. Talavera, T. Voets, B. Nilius, Permeation and selectivity of TRP channels, Annu. Rev. Physiol. 68 (2006) 685–717.
[4] I. Alvarez-Miguel, P. Cidad, M.T. Perez-Garcia, J.R. Lopez-Lopez, Differences in TRPC3 and TRPC6 channels assembly in mesenteric vascular smooth muscle cells in essential hypertension, J. Physiol. 595 (5) (2017) 1497–1513.
[5] M. Mederos, Y. Schnitzler, U. Storch, S. Meibers, P. Nurwakagari, A. Breit, K. Essin, M. Gollasch, T. Gudermann, G_q-coupled receptors as mechanosensors mediating myogenic vasoconstriction, EMBO J. 27 (23) (2008) 3092–3103.
[6] S. Earley, T.J. Heppner, M.T. Nelson, J.E. Brayden, TRPV4 forms a novel Ca^{2+} signaling complex with ryanodine receptors and B_{KCa} channels, Circ. Res. 97 (12) (2005) 1270–1279.
[7] S. Earley, T. Pauyo, R. Drapp, M.J. Tavares, W. Liedtke, J.E. Brayden, TRPV4-dependent dilation of peripheral resistance arteries influences arterial pressure, Am. J. Physiol. Heart Circ. Physiol. 297 (3) (2009) (H1096–102).
[8] D.M. Bautista, P. Movahed, A. Hinman, H.E. Axelsson, O. Sterner, E.D. Hogestatt, D. Julius, S.E. Jordt, P.M. Zygmunt, Pungent products from garlic activate the sensory ion channel TRPA1, Proc. Natl. Acad. Sci. U. S. A. 102 (34) (2005) 12248–12252.
[9] L.H. Wang, M. Luo, Y. Wang, J.J. Galligan, D.H. Wang, Impaired vasodilation in response to perivascular nerve stimulation in mesenteric arteries of TRPV1-null mutant mice, J. Hypertens. 24 (12) (2006) 2399–2408.
[10] Y. Li, R.L. Baylie, M.J. Tavares, J.E. Brayden, TRPM4 channels couple purinergic receptor mechanoactivation and myogenic tone development in cerebral parenchymal arterioles, J. Cereb. Blood Flow Metab. 34 (10) (2014) 1706–1714.
[11] C.J. Garland, S.V. Smirnov, P. Bagher, C.S. Lim, C.Y. Huang, R. Mitchell, C. Stanley, A. Pinkney, K.A. Dora, TRPM4 inhibitor 9-phenanthrol activates endothelial cell intermediate conductance calcium-activated potassium channels in rat isolated mesenteric artery, Br. J. Pharmacol. 172 (4) (2015) 1114–1123.
[12] C.M. Hecquet, G.U. Ahmmed, S.M. Vogel, A.B. Malik, Role of TRPM2 channel in mediating H_2O_2-induced Ca^{2+} entry and endothelial hyperpermeability, Circ. Res. 102 (3) (2008) 347–355.
[13] A. Zholos, Pharmacology of transient receptor potential melastatin channels in the vasculature, Br. J. Pharmacol. 159 (8) (2010) 1559–1571.
[14] C. Grimm, R. Kraft, S. Sauerbruch, G. Schultz, C. Harteneck, Molecular and functional characterization of the melastatin-related cation channel TRPM3, J. Biol. Chem. 278 (24) (2003) 21493–21501.
[15] N. Lee, J. Chen, L. Sun, S. Wu, K.R. Gray, A. Rich, M. Huang, J.H. Lin, J.N. Feder, E.B. Janovitz, P.C. Levesque, M.A. Blanar, Expression and characterization of human transient receptor potential melastatin 3 (hTRPM3), J. Biol. Chem. 278 (23) (2003) 20890–20897.
[16] J. Oberwinkler, S.E. Philipp, TRPM3, Handb. Exp. Pharmacol. 222 (2014) 427–459.
[17] J. Naylor, J. Li, C.J. Milligan, F. Zeng, P. Sukumar, B. Hou, A. Sedo, N. Yuldasheva, Y. Majeed, D. Beri, S. Jiang, V.A. Seymour, L. McKeown, B. Kumar, C. Harteneck, D. O'Regan, S.B. Wheatcroft, M.T. Kearney, C. Jones, K.E. Porter, D.J. Beech, Pregnenolone sulphate- and cholesterol-regulated TRPM3 channels coupled to vascular smooth muscle secretion and contraction, Circ. Res. 106 (9) (2010) 1507–1515.
[18] K. Held, T. Kichko, K. De Clercq, H. Klaassen, R. Van Bree, J.C. Vanherck, A. Marchand, P.W. Reeh, P. Chaltin, T. Voets, J. Vriens, Activation of TRPM3 by a potent synthetic ligand reveals a role in peptide release, Proc. Natl. Acad. Sci. U. S. A. 112 (11) (2015) E1363–E1372.
[19] J. Vriens, G. Owsianik, T. Hofmann, S.E. Philipp, J. Stab, X. Chen, M. Benoit, F. Xue, A. Janssens, S. Kerselaers, J. Oberwinkler, R. Vennekens, T. Gudermann, B. Nilius, T. Voets, TRPM3 is a nociceptor channel involved in the detection of noxious heat, Neuron 70 (3) (2011) 482–494.
[20] S. Hughes, C.A. Pothecary, A. Jagannath, R.G. Foster, M.W. Hankins, S.N. Peirson, Profound defects in pupillary responses to light in TRPM-channel null mice: a role for TRPM channels in non-image-forming photoreception, Eur. J. Neurosci. 35 (1) (2012) 34–43.
[21] T.F. Wagner, S. Loch, S. Lambert, I. Straub, S. Mannebach, I. Mathar, M. Dufer, A. Lis, V. Flockerzi, S.E. Philipp, J. Oberwinkler, Transient receptor potential M3 channels are ionotropic steroid receptors in pancreatic beta cells, Nat. Cell Biol. 10 (12) (2008) 1421–1430.
[22] H.C. Chen, J. Xie, Z. Zhang, L.T. Su, L. Yue, L.W. Runnels, Blockade of TRPM7 channel activity and cell death by inhibitors of 5-lipoxygenase, PLoS One 5 (6) (2010) e11161.

[23] R.A. Nicholas, W.C. Watt, E.R. Lazarowski, Q. Li, K. Harden, Uridine nucleotide selectivity of three phospholipase C-activating P_2 receptors: identification of a UDP-selective, a UTP-selective, and an ATP- and UTP-specific receptor, Mol. Pharmacol. 50 (2) (1996) 224–229.
[24] S.D. Brain, A.D. Grant, Vascular actions of calcitonin gene-related peptide and adrenomedullin, Physiol. Rev. 84 (3) (2004) 903–934.
[25] F.A. Russell, R. King, S.J. Smillie, X. Kodji, S.D. Brain, Calcitonin gene-related peptide: physiology and pathophysiology, Physiol. Rev. 94 (4) (2014) 1099–1142.
[26] F. Van Valen, G. Piechot, H. Jurgens, Calcitonin gene-related peptide (CGRP) receptors are linked to cyclic adenosine monophosphate production in SK-N-MC human neuroblastoma cells, Neurosci. Lett. 119 (2) (1990) 195–198.
[27] H.G. Knaus, O.B. McManus, S.H. Lee, W.A. Schmalhofer, M. Garcia-Calvo, L.M. Helms, M. Sanchez, K. Giangiacomo, J.P. Reuben, A.B. Smith 3rdet al., Tremorgenic indole alkaloids potently inhibit smooth muscle high-conductance calcium-activated potassium channels, Biochemistry 33 (19) (1994) 5819–5828.
[28] J.P. Felix, R.M. Bugianesi, W.A. Schmalhofer, R. Borris, M.A. Goetz, O.D. Hensens, J.M. Bao, F. Kayser, W.H. Parsons, K. Rupprecht, M.L. Garcia, G.J. Kaczorowski, R.S. Slaughter, Identification and biochemical characterization of a novel nortriterpene inhibitor of the human lymphocyte voltage-gated potassium channel, $K_V1.3$, Biochemistry 38 (16) (1999) 4922–4930.
[29] P. Escoubas, S. Diochot, M.L. Celerier, T. Nakajima, M. Lazdunski, Novel tarantula toxins for subtypes of voltage-dependent potassium channels in the K_V2 and K_V4 subfamilies, Mol. Pharmacol. 62 (1) (2002) 48–57.
[30] Z. Yue, J. Xie, A.S. Yu, J. Stock, J. Du, L. Yue, Role of TRP channels in the cardiovascular system, Am. J. Physiol. Heart Circ. Physiol. 308 (3) (2015) H157–H182.
[31] C. Harteneck, Pregnenolone sulfate: from steroid metabolite to TRP channel ligand, Molecules 18 (10) (2013) 12012–12028.
[32] V. Meseguer, Y.A. Alpizar, E. Luis, S. Tajada, B. Denlinger, O. Fajardo, J.A. Manenschijn, C. Fernandez-Pena, A. Talavera, T. Kichko, B. Navia, A. Sanchez, R. Senaris, P. Reeh, M.T. Perez-Garcia, J.R. Lopez-Lopez, T. Voets, C. Belmonte, K. Talavera, F. Viana, TRPA1 channels mediate acute neurogenic inflammation and pain produced by bacterial endotoxins, Nat. Commun. 5 (2014) 3125.
[33] D.W. Gray, I. Marshall, Human alpha-calcitonin gene-related peptide stimulates adenylate cyclase and guanylate cyclase and relaxes rat thoracic aorta by releasing nitric oxide, Br. J. Pharmacol. 107 (3) (1992) 691–696.
[34] X. Yu, F. Li, E. Klussmann, J.N. Stallone, G. Han, G protein-coupled estrogen receptor 1 mediates relaxation of coronary arteries via cAMP/PKA-dependent activation of MLCP, Am. J. Physiol. Endocrinol. Metab. 307 (4) (2014) E398–E407.
[35] J.G. De Mey, R. Megens, G.E. Fazzi, Functional antagonism between endogenous neuropeptide Y and calcitonin gene-related peptide in mesenteric resistance arteries, J. Pharmacol. Exp. Ther. 324 (3) (2008) 930–937.
[36] R. Aoki, U. Yokoyama, Y. Ichikawa, M. Taguri, S. Kumagaya, R. Ishiwata, C. Yanai, S. Fujita, M. Umemura, T. Fujita, S. Okumura, M. Sato, S. Minamisawa, T. Asou, M. Masuda, S. Iwasaki, S. Nishimaki, K. Seki, S. Yokota, Y. Ishikawa, Decreased serum osmolality promotes ductus arteriosus constriction, Cardiovasc. Res. 104 (2) (2014) 326–336.
[37] A. Drews, F. Mohr, O. Rizun, T.F. Wagner, S. Dembla, S. Rudolph, S. Lambert, M. Konrad, S.E. Philipp, M. Behrendt, S. Marchais-Oberwinkler, D.F. Covey, J. Oberwinkler, Structural requirements of steroidal agonists of transient receptor potential melastatin 3 (TRPM3) cation channels, Br. J. Pharmacol. 171 (4) (2014) 1019–1032.
[38] J. Oberwinkler, A. Lis, K.M. Giehl, V. Flockerzi, S.E. Philipp, Alternative splicing switches the divalent cation selectivity of TRPM3 channels, J. Biol. Chem. 280 (23) (2005) 22540–22548.
[39] U. Krugel, I. Straub, H. Beckmann, M. Schaefer, Primidone inhibits TRPM3 and attenuates thermal nociception in vivo, Pain 158 (5) (2017) 856–867.
[40] I. Straub, U. Krugel, F. Mohr, J. Teichert, O. Rizun, M. Konrad, J. Oberwinkler, M. Schaefer, Flavanones that selectively inhibit TRPM3 attenuate thermal nociception in vivo, Mol. Pharmacol. 84 (5) (2013) 736–750.
[41] G. Santoni, C. Cardinali, M.B. Morelli, M. Santoni, M. Nabissi, C. Amantini, Danger- and pathogen-associated molecular patterns recognition by pattern-recognition receptors and ion channels of the transient receptor potential family triggers the inflammasome activation in immune cells and sensory neurons, J. Neuroinflammation 12 (2015) 21.
[42] B. Boonen, Y.A. Alpizar, V.M. Meseguer, K. Talavera, TRP channels as sensors of bacterial endotoxins, Toxins (Basel) 10 (8) (2018).
[43] B. Boonen, Y.A. Alpizar, A. Sanchez, A. Lopez-Requena, T. Voets, K. Talavera, Differential effects of lipopolysaccharide on mouse sensory TRP channels, Cell Calcium 73 (2018) 72–81.
[44] M. Eberhardt, M. Dux, B. Namer, J. Miljkovic, N. Cordasic, C. Will, T.I. Kichko, J. de la Roche, M. Fischer, S.A. Suarez, D. Bikiel, K. Dorsch, A. Leffler, A. Babes, A. Lampert, J.K. Lennerz, J. Jacobi, M.A. Marti, F. Doctorovich, E.D. Hogestatt, P.M. Zygmunt, I. Ivanovic-Burmazovic, K. Messlinger, P. Reeh, M.R. Filipovic, H2S and NO cooperatively regulate vascular tone by activating a neuroendocrine HNO-TRPA1-CGRP signalling pathway, Nat. Commun. 5 (2014) 4381.
[45] M.N. Sullivan, A.L. Gonzales, P.W. Pires, A. Bruhl, M.D. Leo, W. Li, A. Oulidi, F.A. Boop, Y. Feng, J.H. Jaggar, D.G. Welsh, S. Earley, Localized TRPA1 channel Ca^{2+} signals stimulated by reactive oxygen species promote cerebral artery dilation, Sci. Signal. 8 (358) (2015) (ra2).
[46] D.J. Cavanaugh, A.T. Chesler, A.C. Jackson, Y.M. Sigal, H. Yamanaka, R. Grant, D. O'Donnell, R.A. Nicoll, N.M. Shah, D. Julius, A.I. Basbaum, *Trpv1* reporter mice reveal highly restricted brain distribution and functional expression in arteriolar smooth muscle cells, J. Neurosci. 31 (13) (2011) 5067–5077.
[47] A. Czikora, I. Rutkai, E.T. Pasztor, A. Szalai, R. Porszasz, J. Boczan, I. Edes, Z. Papp, A. Toth, Different desensitization patterns for sensory and vascular TRPV1 populations in the rat: expression, localization and functional consequences, PLoS One 8 (11) (2013) e78184.
[48] S. Earley, A.L. Gonzales, R. Crnich, Endothelium-dependent cerebral artery dilation mediated by TRPA1 and Ca^{2+}-activated K^+ channels, Circ. Res. 104 (8) (2009) 987–994.
[49] T. Kark, Z. Bagi, E. Lizanecz, E.T. Pasztor, N. Erdei, A. Czikora, Z. Papp, I. Edes, R. Porszasz, A. Toth, Tissue-specific regulation of microvascular diameter: opposite functional roles of neuronal and smooth muscle located vanilloid receptor-1, Mol. Pharmacol. 73 (5) (2008) 1405–1412.
[50] X. Qian, M. Francis, V. Solodushko, S. Earley, M.S. Taylor, Recruitment of dynamic endothelial Ca^{2+} signals by the TRPA1 channel activator AITC in rat cerebral arteries, Microcirculation 20 (2) (2013) 138–148.